J. Coat. Technol. Res.
https://doi.org/10.1007/s11998-021-00482-0

The influence of barrier pigments in waterborne barrier coatings on cellulose nanofiber layers

Mohammed Al-Gharrawi, Rachel Ollier, Jinwu Wang, Douglas W. Bousfield

Received: 10 November 2020 / Revised: 5 February 2021 / Accepted: 7 February 2021

Abstract Layers of cellulose nanofibers (CNF) have great potential to be used in food packaging applications because of their oxygen and grease barrier properties. However, because of their sensitivity to moisture, they likely will need to be used in a layered structure with water vapor barrier layers. Waterborne barrier coatings (WBBC) have the potential to provide this water vapor barrier, but their performance on paper with a CNF layer has not been described in the literature. Paper that had a CNF layer was coated with three different WBBC with various levels of two different barrier pigments to improve the water vapor barrier properties of these systems. The effective diffusion coefficient of these systems was obtained by fitting the data to a two-layer diffusion model. A finite element code was used to predict the flux rate of water vapor through the barrier layers in the presence of a barrier pigment. The dangers of samples ''blocking'' in production have been tested as well as grease barrier properties. The presence of the CNF layer on paper is shown to improve the performance of the water vapor barrier layer, in some cases, by a factor of six. Adding barrier pigment to the WBBC improves barrier properties at low concentration by 15%, but as the concentration of pigment increases, the barrier properties decrease. The water vapor transmission rate does not decrease to the same order of magnitude as expected from simple theoretical models and the finite element calculations. This result likely is linked to fine bubbles in the coatings that are hard to remove or other defects that are generated during coating or drying. Barrier pigments remove concerns around blocking. All samples had good grease barrier properties.

Keywords Cellulose nanofibers, Barrier pigments, Waterborne barrier coatings, Barrier properties, Food packaging, Finite element model

Introduction

Because of the demand for packaging that can be recycled and will break down in the environment, research into cellulose-based packaging systems is important. Many current packaging systems, such as snack packaging, are composed of two or three different polymers laminated together in three or more layers with a metal layer.[1] These packages are difficult to recycle and will persist in the environment for decades. Cellulose nanofibers (CNF), also in some literature called microfibrillated cellulose, are a promising material that could be used in food packaging, not only because of their high oxygen and grease barrier properties and low costs, but also because CNF is a sustainable and environmentally friendly alternative to petrochemical-based coatings or metalized layers.[2,3] However, a path forward as to how to use CNF in a packaging system is not clear.

CNF layers are of high interest because they are low cost, should be able to be recycled with paper, sequester carbon if put in a landfill, and do break down in the environment. Reviews of the recent literature describing cellulose nanomaterials are given by Moon et al.[4,5] Literature reviews of the use of

This paper was presented at the 2020 International Society of Coatings Science and Technology Conference that was held virtually September 20–23, 2020.

M. Al-Gharrawi, R. Ollier, D. W. Bousfield (✉)
Paper Surface Science Program, Department of Chemical and Biomedical Engineering, University of Maine, Jennens Hall, Orono, ME 04469, USA
e-mail: bousfld@maine.edu

J. Wang
Forest Products Laboratory, U.S. Forest Service, 1 Gifford Pinchot Drive, Madison, WI 53726, USA

Published online: 04 May 2021

cellulose nanomaterials in packaging are given by several researchers.[2,3,6]

The use of biopolymers in packaging is also of high interest, but these materials have potential difficulties. A general review of biologically sourced materials and biopolymers for packaging was given by Johansson et al.[7] and Rastogi and Samyn.[8] While a number of biopolymers are of interest, introducing a new biopolymer into the recycling system could cause issues with recycling.[9] While many biopolymers are compostable in industrial composting facilities, they may not always break down in ocean conditions.[10]

CNF films have been shown to have good barrier properties for oxygen.[2] However, they are not appropriate barrier layers for water vapor and lose their oxygen barrier properties in high humidity. Lavoine et al.,[2] Wang et al.,[11] and Nair et al.[12] reviewed water and oxygen barrier properties of CNF films; these films are often a factor of 100 times more effective as an oxygen barrier compared to standard polymers such as polyethylene (PE).[11] However, the water vapor barrier properties are poor compared to standard polymer films such as PE. Aulin et al.[13] reported oxygen permeabilities of less than 0.001 $cm^3/(m^2$ day kPa) and grease proof property at low humidities, but special treatment is needed to obtain these properties at high humidities. Another form of CNF, called TEMPO mediated oxidized CNF, is also known to have good oxygen barrier properties but is also sensitive to moisture. Fukuzumi et al.[14] and Kumar et al.[15] compared the oxygen barrier properties of different CNF forms; even the low-quality CNF produced with a refiner had low oxygen permeability with a value of 2 $cm^3/(m^2$ day) at low humidity.

The production of stand-alone CNF films is possible using standard coating techniques: a CNF suspension at low solids is coated onto a plastic carrier layer and then peeled away after drying.[16] This method produces a semi-transparent film that is similar to standard polymeric films, but this process may be difficult to implement at high speeds because of the drying requirements of the process. Another option is to coat CNF onto paper, to form a continuous layer on top of the paper surface. Recently, several researchers[16–21] showed that this is possible using blade or rod coating methods, a secondary headbox on the wet end of the paper machine, and slot-die coating methods: cross sections of the paper samples show a dense CNF layer on top of a porous paper surface. In addition, the blade coating of CNF onto a paper web has been demonstrated at high speeds.[18] Therefore, it seems practical to produce a paper that has a dense layer of CNF on at least one side.

The fundamental hypothesis that motivates this work is that a CNF layer will be an effective oxygen barrier layer even at high humidity if it is sandwiched between coatings that have good water vapor barrier behavior. Any water vapor barrier layer that can break down in the environment and not influence paper recycling processes is of interest. Extruded polymer films may be needed for some products to obtain the required barrier properties, but WBBC are preferred because they can be applied at high speeds and do not interfere with the paper recycling system.[22,23]

Therefore, one path toward a new packaging system would be a layered structure that involves paper and a CNF layer that are sandwiched together by two water vapor barrier layers, as depicted in Fig. 1. Hubbe et al.[24] reviewed the various approaches reported in the literature to use protective layers to water vapor with a CNF layer; most of these approaches involve a wax or polymer film. Österberg et al.[25] showed that a wax treatment to the CNF surface helped improve the oxygen barrier even at 90% humidity. Chinga-Carrasco et al.[26] reported on the oxygen barrier properties of layered structures. Recently, polylactic acid (PLA) was used as a water vapor barrier with a layer CNF: excellent oil, oxygen, and water vapor barrier properties were obtained by the extrusion coating of PLA onto a CNF coated paper.[27] However, PLA may cause issues in recycling systems and may not break down in ocean conditions.[10] The behavior of a WBBC on a CNF layer is not reported in the literature.

WBBC have great potential to provide the water barrier needed in packaging because they can be applied at high speeds and are considered environmentally friendly.[28] A number of previous researchers have reported on the influence of polymer type and barrier pigment properties on the barrier properties of these coatings on paper.[22,23,28–31] Recently, Zhu et al.[32] reviewed past work and reported on the change in barrier properties after folding. Martinez-Hermosilla et al.[33] reviewed various expressions for the influence of barrier pigment concentration and shape in barrier coatings. WBBC have challenges because of the potential for pinholes and the occurrence of blocking after production. While barrier pigments do improve the barrier properties, the improvement is often limited and less than what may be expected. There remains a need to better understand how barrier pigments influence the final barrier properties and how these coatings perform on paper that has a CNF layer.

In this work, the barrier properties of paper with a layer of CNF on one side that is coated with three types of WBBC with two different barrier pigments at various pigment content are reported. Samples were coated on both sides of the paper. The water vapor transmission rate (WVTR) was obtained for a range of

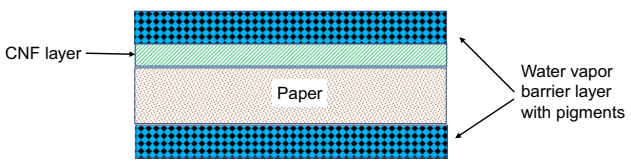

Fig. 1: Concept of layered structure with CNF layer to give grease, oxygen barrier, and outside layer to give water vapor barrier. The water vapor barrier layers are composed of polymers and pigments that should protect the CNF layer from moisture to retain its oxygen barrier properties

coat weights for each polymer-pigment combination. An effective diffusion coefficient of the barrier layer was found by fitting the data to a two-layer diffusion model. A commercial finite element code was used to predict the diffusion of water through the barrier layer in the presence of barrier pigments: results are compared to the experimental data. The grease resistance and blocking tendency are also reported.

Materials and methods

Barrier coatings were applied on paper made at the Process Development Center at the University of Maine. The base paper is 80 g/m^2 basis weight and has a top layer of CNF at 4 g/m^2. The base sheet was an 80:20 hardwood: softwood blend. The paper was manufactured on a pilot paper machine, which consists of a Fourdrinier forming section, press section, and drying section. The CNF used in this study was produced from bleached softwood Kraft pulp by two-stage disk refining at 3% consistency, to a fine content of 90% as measured on a fiber size analyzer (MorFI, Techpap Inc.). The CNF has a large number of fibers that are on the order of 50 nm in diameter and 5 μm in length, but there is a large size distribution of material.

The surface application of CNF on paper was achieved via an in-house built secondary headbox. A dilute suspension (0.5% by weight) flows from this headbox, forms a curtain, and deposits on the wet paper web. The web goes through the standard press and drying sections of the machine. The CNF coated paper had a low air permeability compared to the base paper without the CNF layer: the permeability coefficients were on the order of 10^{-14} and 10^{-16} m^2 for the uncoated and coated paper, respectively. The rate of water uptake for the coated paper was over ten times slower than the uncoated paper. More details about the method to produce the paper are given in Johnson et al.[18]

Three different waterborne barrier coatings based on different polymers were used in this work named polymer A, B, and C. Polymer A was supplied by Mantrose-Haeuser titled VerdeCoat WB-10 for A_1 and WB-10-base for A_2. This material is FDA approved for food contact and is expected to meet standards for compostability. Before application, it has a solid content of 36.5% and a density of 1.03 g/cm^3. Polymer B was supplied by OMNOVA Solutions titled X12-185; it has a solid content of 52% and is a styrene-butadiene latex-based chemistry with a particle size of 180–220 nm and a glass transition temperature of 5°C. It serves as a water, grease, and moisture vapor barrier coating. Polymer C was supplied by Michelman (Michem Prime 4983R). The chemical nature of the preparation is ethylene-acrylic acid dispersion and is a translucent liquid that has a solid content of 24.8%.

Two barrier pigments were used in the barrier coating formulation. Kaolin was supplied by Imerys Minerals Ltd. (Barrisurf HX); it has a 64% particle size less than 2 μm and a shape factor, linked to the aspect ratio, of over 90. The second pigment used in this work was a bentonite clay (PGN, Minerals Technologies). It had a cation-exchange capacity (CEC) of 1.2 meq g^{-1} and moisture content of 12%, respectively. The aspect ratio was 300–500, and the thickness is on the order of 10 nm, according to the manufacturer.

The coating process was performed using a laboratory bench-size automatic rod coater (model 21001, BYK Gardner USA) with standard Mayer Rods. Different rod size and pressure were used to end up with different amounts of the coating. For the low coat weight level, the rod size and pressure knob are #3 and 6.5; for moderate coat weight they are #5 and 7; and for high coat weights, they are #7 and 7.5. The speed was fixed at 6.1 m/min. To ensure that the coating weight on both sides is similar, for a number of samples, the coat weight on each side was determined separately. The coat weights were within 5% in these tests. The CNF side was coated first.

Coatings were dried at 105°C for 5 min except for a few samples with polymer A that were dried at 125°C for comparison. All samples were coated on both sides, where the first side is dried before the second coating was applied. The coat weight is determined by measuring the weight change after coating two sides. Polymer A is known to obtain its full cure after drying at 125°C for 2 min in order to obtain its best results. Therefore, a few tests compared this cure temperature with the 105°C conditions.

The water vapor barrier property of the coating was measured according to ASTM 96/E96M-16. In a controlled temperature and humidity room (23°C, 50% relative humidity), jars were filled up with 30 mL of water and closed by the sample of interest as the lid. The sample was held against the jar with a silicone gasket and a metal screw top rim. Samples were conditioned at least one day to avoid any initial changes due to the humidity conditions. The weight change over at least 24 h was used to calculate the WVTR.

Samples were tested for pinholes by applying several drops of colored water for a minute and then wiping them off the sample. The appearance of colored spots indicates more or bigger pinholes. Indigo carmine was used as a dye at a concentration of 10 g/L. Scanning electron microscope (SEM) images were obtained with a benchtop device (Hitachi, TM 3000).

The grease barrier properties were determined with TAPPI method (T559 cm-02) based on 12 different solutions numbered from 1 to 12 nominated as a Kit Test number. This test was developed to rate the performance of fluoro-chemical treated papers, but it is now often used as an initial indication of a sample's resistance to grease or oil penetration for food packaging. These solutions are made of different ratios of castor oil, n-heptane, and toluene. The solution number one represents the least aggressive, with the smallest surface energy, viscosity, and contact angle

on the test paper surface, while the solution number twelve is the most aggressive. Drops of the solutions were dropped on a sample from a height of 40 mm. After 15 s, they were removed using tissue paper, and each analysis was made at least five times for each sample.

The blocking test is performed with a heated press. The coated side was pressed against another coated surface for 6 h at the temperature of 50°C and the pressure of 0.5 MPa. After the samples had cooled, they were detached from each other, and the blocking tendency was evaluated according to five levels, as shown in Table 1, ordered from not attached level to totally attached, with three other levels between.

Theory and modeling

By assuming that water vapor transmission in paper and coatings follows Fick's law and steady-state conditions, the standard equation to predict the total flux of water vapor or the WVTR for two layers can be written as:

$$\mathrm{WVTR} = \frac{M_w(C_o - C_1)}{\left(\frac{H_p}{D_p} + \frac{H_c}{D_c}\right)} \quad (1)$$

M_w is the molecular weight of water, C_o and C_1 are the concentration of water vapor inside and outside of the jar, respectively, H_p and H_C are the thicknesses of the paper and coating layer, respectively, and D_P and D_c are the effective diffusion coefficients of the paper and coating, respectively. The partition coefficient of water and polymer is assumed to be constant and becomes included with the diffusion coefficient. While the barrier coating layer is actually on each side of the sample, equation (1) predicts the same behavior where the coating thickness is the sum of the two coating layer thicknesses and the CNF-paper layers are considered as a single layer. Using the vapor pressure of water at room temperature, the concentration of water vapor inside the jar is 1.1 mol/m^3. The 50% relative humidity would have a concentration of half of this value outside of the jar. The WVTR of the uncoated paper is around 400 g/m^2 day. The thickness of the paper was 0.098 mm. This thickness gives a diffusion coefficient for the paper of 4.6×10^{-8} m^2/s.

A wide range of coat weights is used in the experiments. Equation (1) is used to fit the data, adjusting the diffusion coefficient of the coating layer D_C to minimize the root mean square error. The coat weight of each sample is measured gravimetrically and is used to calculate the coating thickness to be used in equation (1) assuming the density appropriate for the certain pigment volume concentration assuming the density of the polymer and pigments to be 1 g/cm^3 and 2.5 g/cm^3, respectively.

To predict the expected performance of the barrier pigments, a commercial finite element code (COMSOL 5.4 Multiphysics) was used to predict the diffusion rate through a polymeric layer that contains barrier pigments of specific shape and concentration. Simulations were carried out in three dimensions. The physics of ''dilute species'' diffusion was used, specifying a concentration boundary condition on two sides of the simulation domain. The barrier pigments were assumed to be spherical or truncated cylinders, to simulate the disk-like nature of the clays. Figure 2 shows the unit cell for a sphere and disk in cubic packing and the same in body-centered cubic (BCC) packing. The behavior of several unit cells was com-

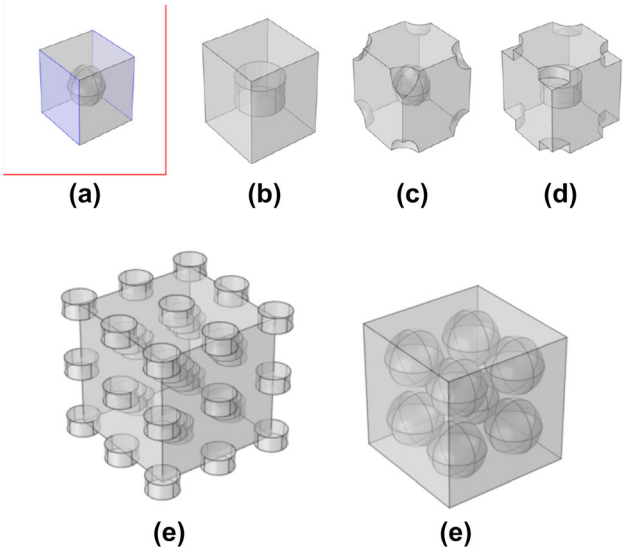

Fig. 2: Examples of unit cells and multi cells (a) cubic packing of a sphere, (b) cubic packing of a disk, (c) BCC packing of spheres, (d) BCC packing of disks, (e) BCC of disks 3 × 3 × 3, and (f) cubic packing of spheres 2 × 2 × 2

Table 1: Ranking system for blocking test

1	Samples not attached
2	Samples attached, but only minor damage and can be easily detached
3	Samples attached, < 50% of the area damaged
4	Samples attached, > 50% of the area damaged
5	Totally blocked

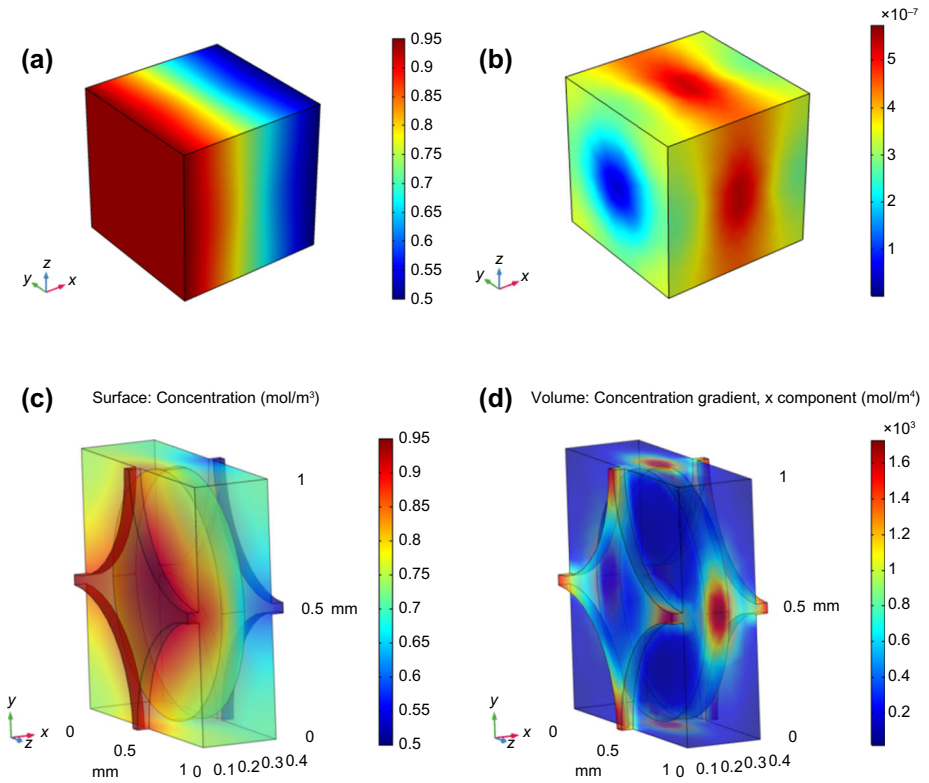

Fig. 3: Sample concentration and flux distributions predicted (a) concentration profile for cubic packing of a sphere, (b) flux distribution for cubic packing of a sphere, (c) concentration profile for BCC packing of a disks, and (d) flux distribution for BCC packing of disks

pared as well, also shown in Fig. 2. The size of the cell relative to the pigment defines the pigment volume concentration (PVC). For high aspect ratio disks, the cell could not be cubic and still allow high values of PVC. For those cases, the disk diameter was set to 96% of the cell unit width and dimension of the cell in the direction of diffusion was adjusted to change PVC. The spheres or disks were ''subtracted'' from the block geometry using the Boolean operation in the program; this subtraction is similar to assuming that the diffusion of water vapor through the mineral is an order of magnitude smaller than that of the polymer. Similar results are obtained if a low diffusion coefficient is assigned to the spheres or disks. The results were checked several times for mesh size. In some cases, over $4 \times 4 \times 4$ geometries of spheres or disks, the code would have some meshing difficulties, but little time was spent to attempt to resolve these because the same results were obtained with simple unit cells.

The total flux of species at one surface is calculated within the code under ''derived values.'' This flux rate is normalized to what happens with no pigment, and an effectiveness factor is defined as:

$$E = J/J_{\mathrm{p}} \tag{2}$$

E ranges from zero up to a value of one for no decrease in flux rate, J is the flux rate predicted with pigments, and J_{p} is the flux rate for the polymer with no pigments. For BCC configurations where the area for diffusion on one surface is reduced due to particles in the corner of the cell, the results were re-normalized to a unit cross-sectional area. Figure 3 shows the concentration profile and the diffusive flux profile of typical calculations for cubic packing for a unit cell for a sphere and BCC packing for a disk-shaped particle with an aspect ratio of ten. Notice that the concentration profile is not disrupted by the presence of the sphere, but the diffusive flux is not uniform: in regions where the cross-sectional area for diffusion is restricted, high flux rates are predicted as expected. For the BCC packing, high flux regions are locations where there is still some passage left for diffusion.

A model of this nature has a number of assumptions. Only the barrier layer was included because the resistance to diffusion of water vapor through the paper-CNF layers is small. In the actual coatings, the pigments are not uniform in size and are not well separated from each other. For the disk-shaped pigments, even though the coating process shear field may help align them perpendicular to the diffusion direction, there will be a distribution of orientations. The model also neglects any defects or nonuniformities of the polymer phase. However, the key purpose of the model is to estimate the expected water vapor transport through these films as barrier pigments are added in an ideal situation.

Results and discussion

The CNF layer on the paper makes a large impact on the effectiveness of the barrier coating applied onto it. The CNF layer on paper with no barrier layer decreases WVTR by 10%. Figure 4 compares the results for polymer A and C when they are coated on both sides for paper with no CNF layer and paper that has a CNF layer. Especially at low coat weights, the CNF layer helps the coating to be over six times more effective. For example, at 10 g/m^2, the WVTR decreases from a value of 120–18 g/m^2 day when one side is applied to the CNF layer. Therefore, the CNF layer must help the coating to stay as a uniform layer on one side of the paper, not allowing it to soak into the paper and become discontinuous. Others have shown cross sections of CNF coated paper that indicate a dense layer on top of the paper that should be able to keep coatings on top as a continuous layer.[17,19] For polymer B, the results are not shown, but the effect of the CNF layer is minor; the high solids content of polymer B is designed to keep it at the paper surface and not penetrate the paper. Therefore, even without the CNF layer, polymer B gives good results.

The lines in Fig. 4 are the fits of equation (1) to the data minimizing the square of the error, where each coat weight represents a specific coating layer thickness. Because of the scatter in the data, the fit of equation (1) is often poor, with R^2 values of less than 0.5, but these model fits allow the trends in the data to be seen and help give an idea as to the effective diffusion coefficient of the coating layer. In some cases, like polymer C, the data do not fit the two-layer model trends. For polymer C on paper, the reason could be that at low coat weights on uncoated paper, the polymer absorbs into the paper structure, not forming a continuous film at all; this results in high WVTR at low coat weights. Once the coat weight increases, a continuous film is generated, and the two-layer model situation is valid. However, when the low coat weight

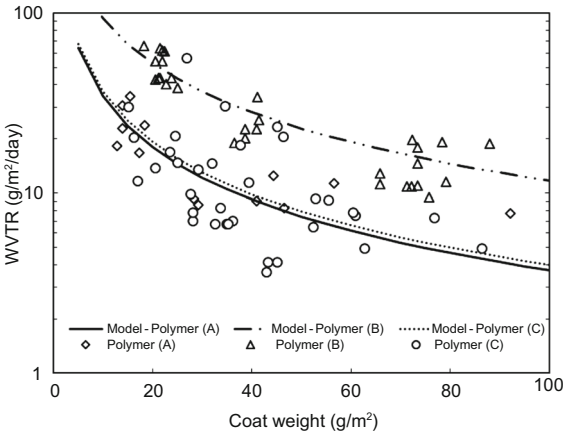

Fig. 5: WVTR for the three polymers with no barrier pigments. Lines are a fit of equation (1) through the data minimizing the root mean square error

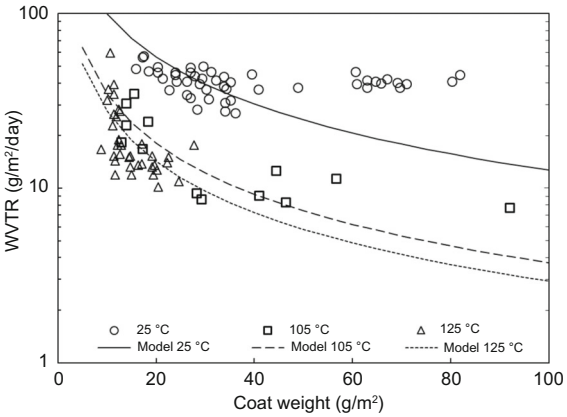

Fig. 6: WVTR of Polymer A dried at various temperatures. Lines are fit of equation (1)

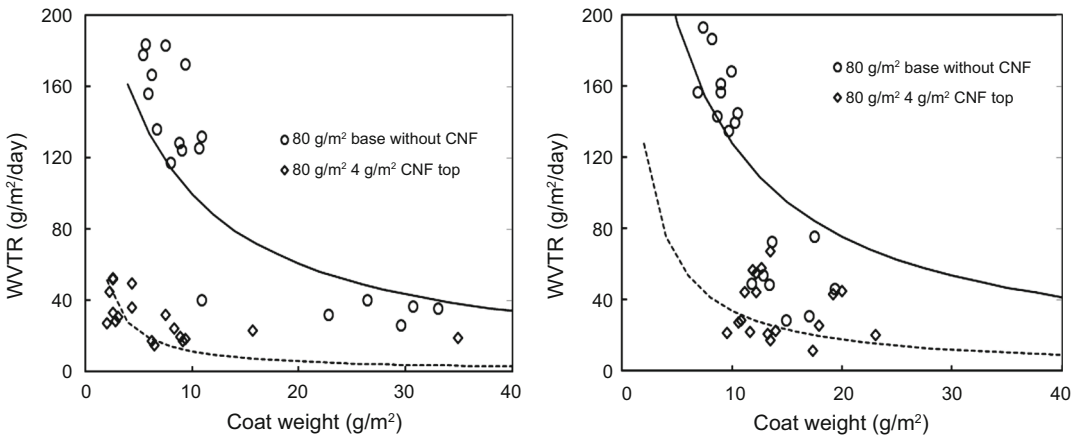

Fig. 4: WVTR of samples for various coat weights of polymer A_1 (left) and polymer C (right) on the base paper and for the same base paper with a CNF layer. Lines are fits to equation (1)

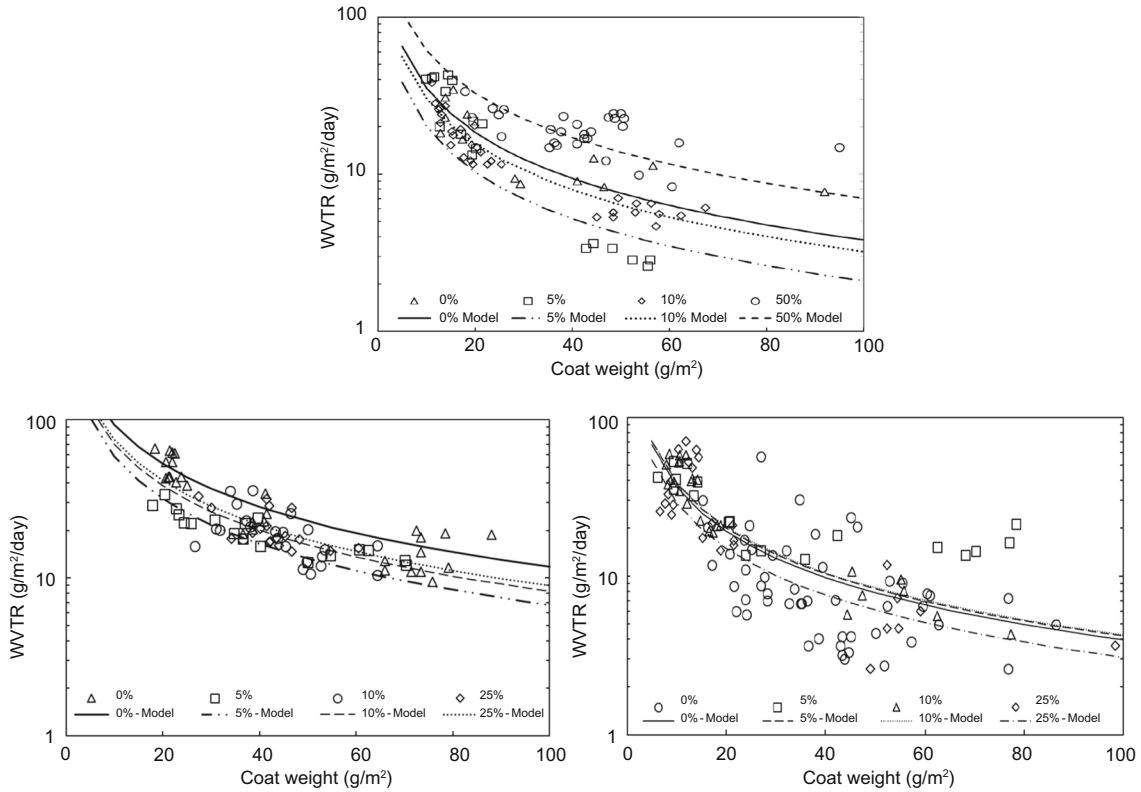

Fig. 7: WVTR for various concentrations of kaolin in polymer A (top), B (left) and polymer C (right). Lines are fitted to equation (1)

data are used in the error minimization, it results in an over prediction of WVTR at high coat weights.

Figure 5 compares the three polymer types with no barrier pigments. As expected, as the coat weight increases, the WVTR decreases. Again, there is significant scatter in the data that likely comes from a number of sources, such as the random occurrence of coating defects, fine defects in the CNF layer, and issues with how the sample seals against the glass jar. Significant effort was made to minimize this scatter, but there must be some random occurrence in the films that causes such a wide scatter. The lines in the figure are fits of equation (1) through the data, adjusting D_c to minimize the error. Polymers A and C give similar results, while polymer B gives, in general, higher results. The difference could be caused by the type of polymer or by a number of other factors such as the surfactants used, solids of the formulation, or the particle size of the polymer component. A number of other factors besides WVTR, such as heat sealing, rheology, and costs, will be important in the final selection of a polymer type. Note the log scale of the vertical axis. The WVTR of some samples are quite small (3 g/m^2 day) compared to what others have reported in the literature at around 60 g/m^2 day for WBBC of similar coat weights on base paper without the CNF layer.[30] Since barrier coatings have a density of 1 g/m^3, 10 g/m^2 of coating would be around 10 mm thick. It should be noted that the total coat weights studied here are likely much higher than what would be practical and economical from an industrial perspective.

The importance of drying temperature for polymer A is shown in Fig. 6. The manufacturer suggests a drying temperature of 125°C. If the samples are dried only at room temperature, WVTR is 100 g/m^2 day and does not improve with increasing the coat weight; this result indicates that the polymer does not form a film when dried at a low temperature. When the sample is dried at 105°C, WVTR decreases to under 10 g/m^2 day at moderate coat weights. When the cure temperature is increased to 125°C, some small improvement is seen, but it seems like the 105°C is enough to obtain reasonable results. To be consistent, all samples with barrier pigments were dried at 105°C.

Similarly, polymer C tends to perform better when applied hot. Fine bubbles seem to be present in the polymer C at room temperature even after careful pouring and mixing of the coating. Increasing the temperature decreases the viscosity that allows bubbles to escape the coating. There was about a 10% improved result for applying at 80°C compared to room temperature.

The influence of the kaolin barrier pigment content on WVTR for all three polymers is reported in Fig. 7. The best results are when kaolin is added at 5% by weight level for polymer A. Some results are in the range of 4 g/m^2 day. However, upon adding more

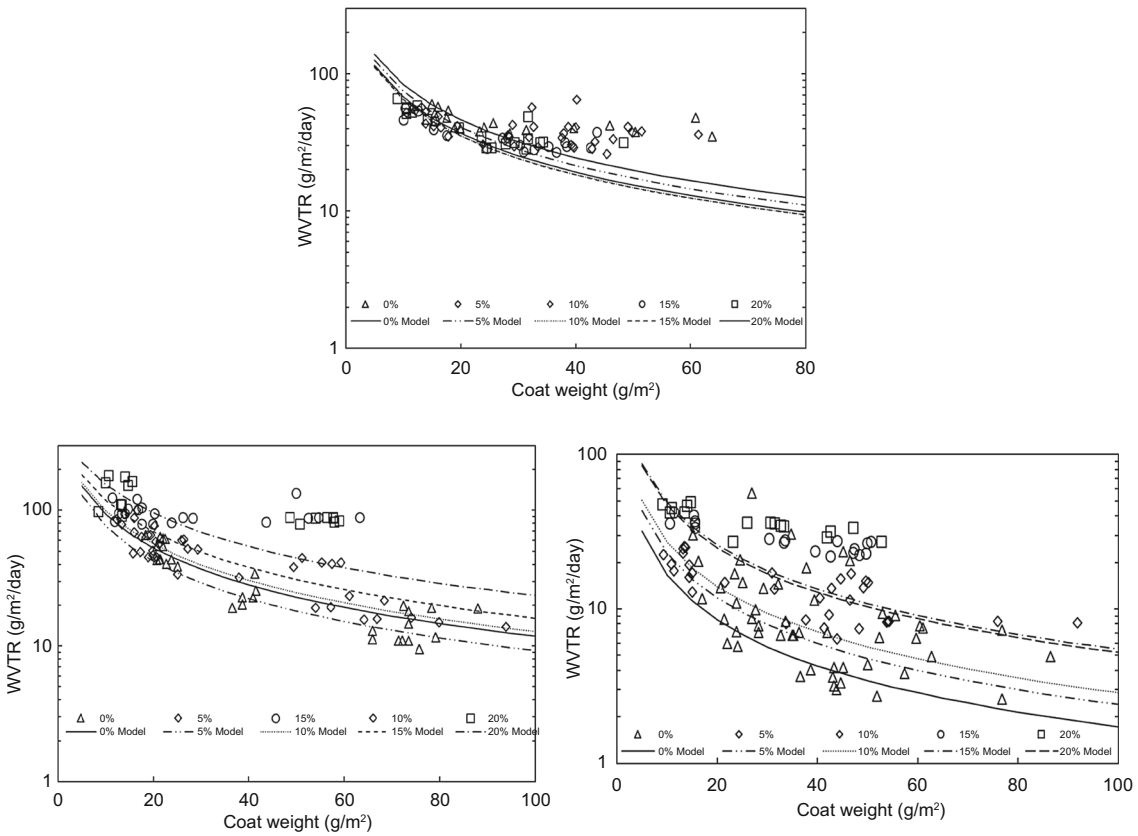

Fig. 8: Effect of Bentonite loading level on WVTR of polymers A (top), B (left) and C (right). Lines are a fit to equation (1)

pigment, the WVTR increases. The reason for this result is not apparent because the critical pigment volume concentration associated with the formation of voids should be at concentrations that are in the range of 50% by weight. Therefore, adding more pigments should decrease WVTR. The same general behavior is seen for all the polymers. This agrees with others in the literature that show a limited improvement of barrier properties with the addition of pigments.[22,23,32] It should be noted that based on the polymer weight used, the barrier pigments do show value. For example, for polymer B, at a coat weight of 40 g/m^2, the coating with barrier pigments performs similar to the pure polymer, yet if the coating is 25% by weight pigment, then that percent would represent the reduction in the polymer use that is expected to be the larger cost driver in this system.

Figure 8 shows the results for the bentonite pigment for polymers A, B, and C. Again, small levels of the pigment improve the barrier results for polymers A and B, but when the weight fraction increases over 15%, then the water transmission rate increases to values larger than the pure polymer. Polymer A at high coat weights does not seem to follow the trends of equation (1). This result may indicate the formation of cracks in the coating layer upon drying or handling even though microscope images did not have clear indications of cracks for these samples. For polymer C, bentonite has a detrimental effect on the results: the WVTR increased related to the pure polymer when the pigment was added on average. Still, the barrier pigments could still be an advantage to use even if there is not a performance increase due to other factors such as cost. The data points show the scatter that is obtained with these samples, especially polymer C. To the eye and touch, these samples look defect-free, but there must be small-scale issues in the coating layer that cause some samples to have much higher WVTR than expected. The scatter must be coming from random defects from sample to sample in the barrier layers caused by air bubbles, cracks, or other issues.

Table 2 compiles the diffusion coefficients obtained by fitting the data. These values seem to be reasonable compared to the results that others have presented.[32] The scatter in the data prevents a closer analysis of the results. For all cases, the surprising result is that the effective diffusion coefficient of the polymer does not steadily decrease as the barrier pigments are added. When the pigment volume concentration is below the critical concentration, more pigments should result in tortuous diffusion paths and limited room for molecules to diffuse in the polymer. Above the critical concentration, air voids will be present, and high diffusion would be expected through these voids.

Table 2: The values of effective moisture diffusion coefficient D_c in coatings obtained from fitting equation (1) for various pigment types and concentrations for polymers A, B, C. Values are in $m^2/s \times 10^{10}$

Polymer	Wt.%										
	Kaolin						Bentonite				
	0	5	10	15	25	50	0	5	10	15	20
A_1	5.1	2.7	–	4.6	–	9.4	–	–	–	–	–
A_2	–	–	–	–	–	–	14	13	12	10	11
B	16	–	9	11	12	19	16	15	20	27	40
C	4.5	6	6.5	–	5.6	–	2.3	3.6	4.5	8.8	9.1

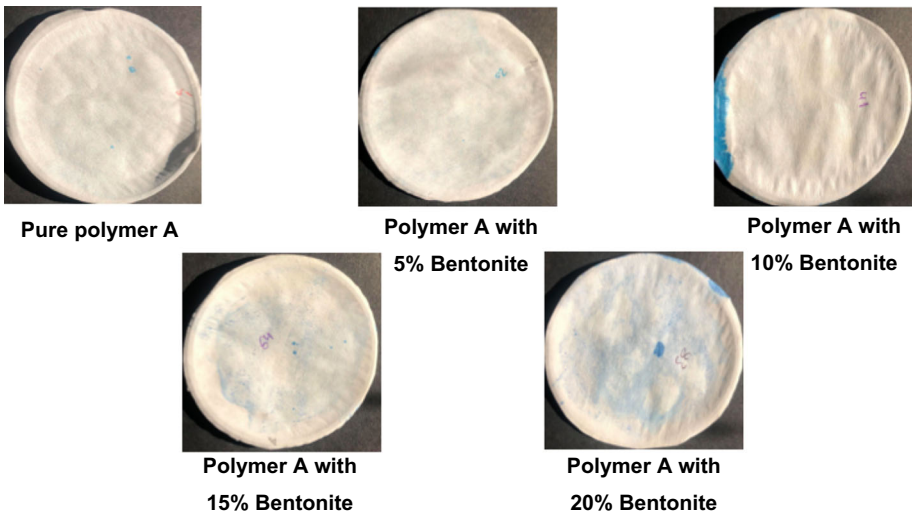

Fig. 9: Pin-hole test for polymer A with bentonite (top) and polymer

However, all of the results presented here should be well below the critical pigment volume concentration value expected when air voids will be present.

By adding drops of dyed water to the surface, it was possible to see pinholes or other defects in the coating layers in some limited situations, but most coatings did not show any defects in this manner. Figure 9 compares the results for bentonite in polymer A at different weight concentrations. Because the dye was water-based, it may not pick-up fine pinholes that are hydrophobic in nature. As the pigment concentration increases, the occurrence of pinholes increases. While these coatings were well mixed and sat in the laboratory for at least 24 h before use, it seems like fine bubbles can persist in the coatings that contain moderate to high levels of pigments. Microscope images suggest spherical defects and not cracks. There are methods to remove air from coatings; these may become important if high levels of pigments are to be used. Figure 10 shows the SEM surface images of the 10% by weight bentonite in polymer C. Again, the defect is spherical in nature, not as a form of cracks. Bollström et al.[22] showed high-resolution SEM images of cross sections that show how defects can occur between barrier pigments.

The predictions of the finite element method are shown in Fig. 11 for spheres and disk particles with an aspect ratio of two and for disk shaped particles of various aspect ratios. A surprising result is that the body-centered packing is not more effective for the sphere case than the cubic packing. Straight paths for diffusion are blocked for BCC packing. However, the packing is more effective at filling up the region with pigments compared to cubic packing resulting in diffusion paths that are less constricted compared to cubic packing. Figure 11 also shows that disk-shaped pigment is more effective as a barrier than spherical pigments as expected. For disk-shaped particles at high PVC, the BCC packing forces E toward zero, but for the cubic packing, the results go to a finite value. This result comes from the open paths for diffusion that are linked to cubic packing, even at high PVC.

For cubic packing of disk-shaped pigments, all of the results are similar to the aspect ratio of the two cases in Fig. 11: the aspect ratio does not influence the values. In all cases, the diffusional direction is perpendicular to

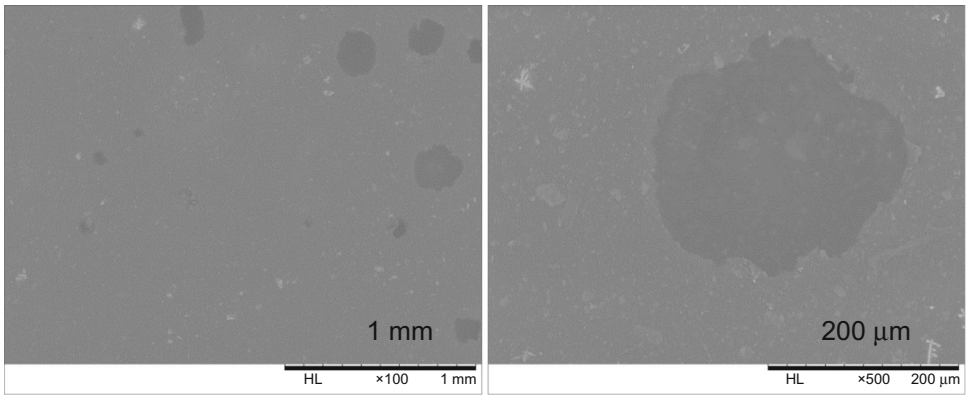

Fig. 10: SEM for a coating of polymer C with 10% bentonite pigment by weight at two magnifications

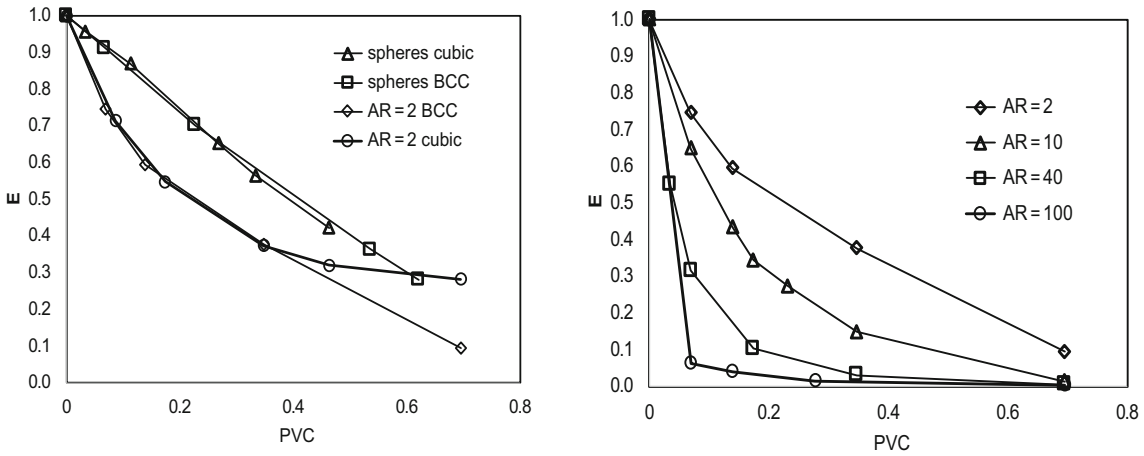

Fig. 11: The influence of PVC on the effectiveness parameter for cubic packed spheres, BCC packed spheres, and BCC packed disks with an aspect ratio (AR) of 2 (left) and as a function of pigment volume concentration for BCC packed disk-shaped particles for aspect ratios of 2, 10, 40, and 100 (right)

the alignment of the disk-shaped particles to represent an idealized case. This result caused by the area available for diffusion is the area of the cell, subtracting a circle. The effective diffusion coefficient scales as this area. However, for BCC of disk particles, a dramatic reduction of diffusion is seen as shown in Fig. 11. This is caused by the destruction of straight paths through the structure and the constricted diffusion paths. The large gradients of flux are seen in Fig. 3.

The results in Fig. 11 are close to the simple expression given by Nielsen[34]

$$E = \frac{(1-\phi)}{(1+\alpha\phi)} \tag{3}$$

ϕ is the pigment volume concentration and α is the aspect ratio of the pigment. Of all of the expressions reported by Martinez-Hermosilla et al.,[33] this simple expression follows all of the BCC packed results within 10%. Therefore, equation (3) seems like an easy prediction tool to look for the potential of barrier pigments.

The change in the flux rate predicted by the model compared to the experimental results is shown in Fig. 12 for the kaolin pigment using equation (2) with an aspect ratio of 100 to show the theoretical results. The key point is that the barrier pigments seem to have the correct drop at PVC around 5%, but afterward, the barrier performance is much less than what would be predicted. Of course, the predicted results are for an idealized case with no cracks or pinholes, pigments all arranged parallel to the surface, and the pigments would be dispersed in the polymer. The experiments are limited in terms of how well the pigments were dispersed, the ability to remove air from the coatings, and the uniformity of the coating applied with the wire wound rods. As discussed above, as PVC increases, the occurrence of defects tends to increase, which canceled the barrier effect of the added pigment. The important message of Fig. 12 is that barrier pigments have a large potential to decrease the WVTR theoretically, but in practice, some mechanisms must be in play that reduce the effectiveness of the pigment. More work is needed to understand what can be done with the coatings in

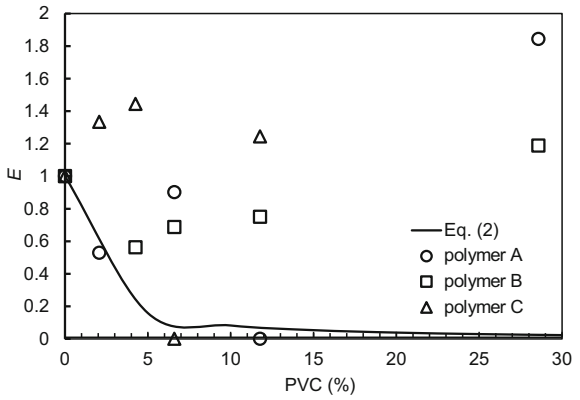

Fig. 12: The effectiveness of the barrier pigment as a function of PVC for the kaolin pigment in three polymers

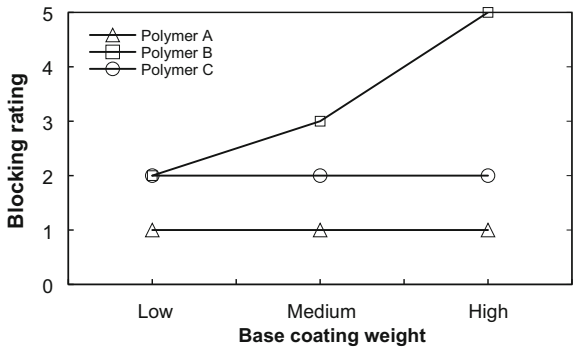

Fig. 13: Blocking test of three levels of coatings for polymers A, B, and C

terms of formulation or processing that can help these barrier pigments realize the predicted potential.

One issue with waterborne barrier coatings is blocking, which is the adhesion of the coating surfaces to other surfaces when rolled up into a cylinder of product. High temperatures are needed to dry and sometimes cure the polymer. After the drier, the web must be rolled up. The warm polymer, at times, can stick the web together in a large block of material. Figure 13 shows the blocking test results for low, medium, and high coat weights. Only at medium and high coat weights did polymer B show some blocking issues. When barrier coating pigments are used at a low and medium level of coatings, all samples had no tendency for blocking, even for the low addition levels of the barrier pigment. Therefore, the barrier pigments play an important role in the reduction of blocking potential.

The barrier coatings also improved the grease barrier properties of the CNF/paper system. For the uncoated CNF paper used before applying a barrier coating, the Kit test number was 4, but the paper only had 4 g/m^2 CNF on it. The paper alone did not have any resistance to oil and did not pass the Kit number of 1. Recent studies with this same CNF showed that coat weights of 8 g/m^2 CNF are needed to provide significant grease barrier properties.[17] Kit test numbers with moderate coat weights of around 20 g/m^2 on each side for A, B, and C are 11, 12, and 8, respectively. For polymers A and B, these values are near the maximum for the test method and are similar to what is obtained to when these coatings are applied to the paper without the CNF layer. Therefore, the grease barrier properties are already excellent for these coatings even without the CNF layer. For polymer C, the kit test value without the CNF layer is 6 compared to 8 with the CNF layer is present; this increase is caused by the barrier properties of these polymers combined with that of the CNF layer. The value of the kit number of these samples was not largely affected by the barrier pigments, even at higher concentration of 25%. These results indicate that the barrier coatings improve the oil/grease resistance of the system and that the barrier pigments do not have a large influence on grease barrier properties.

Conclusions

A CNF layer on paper increases the effectiveness of water-based barrier coatings at low coat weights; the CNF layer may help keep the barrier layer as a continuous layer by not letting it penetrate into the paper structure to be discontinuous. Barrier pigments added to the water-based barrier coating improved the barrier properties a limited amount at low weight fractions. In most cases, the improvement in barrier properties is less than theoretical predictions. The presence of the pigments at moderate levels tended to lead to pinholes or other types of defects. These defects suggest the need for even better mixing and air removal to realize the full benefit of the pigments. Coated samples had excellent grease barrier properties. Except for one system without barrier pigments, blocking problems were minimal.

Acknowledgments This project was funded in part by U.S. Endowment for Forestry and Communities (P^{3}Nano) Grant Number E17-20 and by the University of Maine Paper Surface Science Program (PSSP). The Higher Committee for Education Development Iraq also provided support.

References

1. Schubert, G, Boiron, G, "Hydro Aluminium Deutschland GmbH." Film for Food Packaging. US Patent Application 10/501,319, 2005
2. Lavoine, N, Desloges, I, Dufresne, A, Bras, J, "Microfibrillated Cellulose - Its Barrier Properties and Applications in

Cellulosic Materials: A Review.'' *Carbohydr. Polym.*, **90** (2) 735–764 (2012)
3. Tyagi, P, Lucia, LA, Hubbe, MA, Pal, L, ''Nanocellulose-Based Multilayer Barrier Coatings for Gas, Oil, and Grease Resistance.'' *Carbohydr. Polym.*, **206** 281–288 (2019)
4. Moon, RJ, Schueneman, GT, Simonsen, J, ''Overview of Cellulose Nanomaterials, Their Capabilities, and Applications.'' *JOM*, **68** (9) 2383–2394 (2016)
5. Moon, RJ, Martini, A, Nairn, J, Simonsen, J, ''Cellulose Nanomaterials Review: Structure, Properties, and Nanocomposites.'' *Chem. Soc. Rev.*, **40** (7) 3941–3994 (2011)
6. Henriette, M, Rosa, A, Mattoso, L, ''Nanocellulose in Bio-Based Food Packaging Applications.'' *Ind. Crops Prod.*. **97** 664–671 (2017)
7. Johansson, C, Bras, J, Mondragon, I, Nechita, P, Plackett, D, Šimon, P, Svetec, DG, Virtanen, S, Baschetti, M, Breen, C, ''Renewable Fibers and Bio-Based Materials for Packaging Applications - A Review of Recent Developments.'' *BioResources*, **7** (2) 2506–2552 (2012)
8. Rastogi, V, Samyn, P, ''Bio-Based Coatings for Paper Applications.'' *Coatings*, **5** (4) 887–930 (2015)
9. Soroudi, A, Jakubowicz, I, ''Recycling of Bioplastics, Their Blends and Biocomposites: A Review.'' *Eur. Polym. J.*, **49** (10) 2839–2858 (2013)
10. Emadian, SM, Onay, TT, Demirel, B, ''Biodegradation of Bioplastics in Natural Environments.'' *Waste Management*, **59** 526–536 (2017)
11. Wang, J, Gardner, D, Stark, N, Bousfield, D, Tajvidi, M, Cai, Z, ''Moisture and Oxygen Barrier Properties of Cellulose Nanomaterial-Based Films.'' *ACS Sustain. Chem. Eng.*, **6** (1) 49–70 (2018)
12. Nair, S, Zhu, J, Deng, Y, Ragauskas, A, ''High-Performance Green Barriers Based on Nanocellulose.'' *Sustain. Chem. Process.*, **2** (1) 23 (2014)
13. Aulin, C, Gällstedt, M, Lindström, T, ''Oxygen and Oil Barrier Properties of Microfibrillated Cellulose Films and Coatings.'' *Cellulose*, **17** (3) 559–574 (2010)
14. Fukuzumi, H, Saito, T, Iwata, T, Kumamoto, Y, Isogai, A, ''Transparent and High Gas Barrier Films of Cellulose Nanofibers Prepared by TEMPO-Mediated Oxidation.'' *Biomacromolecules*, **10** (1) 162–165 (2009)
15. Kumar, V, Bollström, R, Yang, A, Chen, Q, Chen, G, Salminen, P, Bousfield, D, Toivakka, M, ''Comparison of Nano- and Microfibrillated Cellulose Films.'' *Cellulose*, **21** (5) 3443–3456 (2014)
16 Peresin, M, Vartiainen, J, Kunnari, V, Kaljunen, T, Tammelin, T, Qvintus, P, ''Large-Scale Nanofibrillated Cellulose Film: An Overview on Its Production, Properties, and Potential Applications.'' In: *Proceeding 4th Int. Conf. Pulping, Papermak. Biotechnol. (ICPPB'12), Vols. I II*, October 2016, pp. 891–895 (2012)
17. Mousavi, S, Afra, E, Tajvidi, M, Bousfield, D, Dehghani-Firouzabadi, M, ''Application of Cellulose Nanofibril (CNF) as Coating on Paperboard at Moderate Solids Content and High Coating Speed Using Blade Coater.'' *Prog. Org. Coat.*, **122** 207–218 (2018)
18. Johnson, D, Paradis, M, Tajvidi, M, Walker, C, Algharrawi M, Bousfield D, ''Surface Application of Cellulose Microfibrils on Paper – Effects of Basis Weight and Surface Coverage Levels.'' In: *Proc. TAPPI PAPERCON Conference*; TAPPI Press (2019)
19. Kumar, V, Elfving, A, Koivula, H, Bousfield, D, Toivakka, M, ''Roll-to-Roll Processed Cellulose Nano Fiber Coatings.'' *Ind. Eng. Chem. Res.*, **55** (12) 3603–3613 (2016)
20. Kumar, V, Koppolu, V, Bousfield, D, Toivakka, M, ''Substrate Role in Coating of Microfibrillated Cellulose Suspensions.'' *Cellulose*, **24** (3) 1247–1260 (2017)
21. Kumar, V, Ottesen, V, Syverud, K, Gregersen, Ø, Toivakka, M, ''Coatability of Cellulose Nanofibril Suspensions: Role of Rheology and Water Retention.'' *BioResources*, **12** 7656–7679 (2017)
22. Bollström, R, Nyqvist, R, Preston, J, Salminen, P, Toivakka, M, ''Barrier Properties Created by Dispersion Coating.'' *Tappi J.*, **12** (4) 45–51 (2013)
23. Vähä-Nissi, M, Savolainen, A, ''Filled Barrier Dispersion Coatings.'' In: *TAPPI Coating Conference*, pp. 287–304 (1999)
24. Hubbe, M, Ferrer, A, Tyagi, P, Yin, Y, Salas, C, Pal, L, Orlando, JR, ''Nanocellulose in Functional Packaging.'' *BioResources*, **12** 2143–2233 (2017)
25. Österberg, M, Vartiainen, J, Lucenius, J, Hippi, U, Seppälä, J, Serimaa, J, Serimaa, R, Laine, JRSJL, ''A Fast Method to Produce Strong NFC Films as a Platform for Barrier and Functional Materials.'' *ACS Appl. Mater. Interfaces,* **5** 4640–4647 (2013)
26. Chinga-Carrasco, G, Averianova, N, Gibadullin, M, Petrov, V, Leirset, I, Syverud, K, ''Micro-Structural Characterisation of Homogeneous and Layered MFC Nano-Composites.'' *Micron*, **44** (1) 331–338 (2013)
27. Koppolu, R, Lahti, J, Abitbol, T, Swerin, A, Kuusipalo, J, Toivakka, M, ''Continuous Processing of Nanocellulose and Polylactic Acid into Multilayer Barrier Coatings.'' *ACS Appl. Mater. Interfaces*, **11** (12) 11920–11927 (2019)
28. Sun, Q, Schork, FJ, Deng, Y, ''Water-Based Polymer/Clay Nanocomposite Suspension for Improving Water and Moisture Barrier in Coating.'' *Compos. Sci. Technol.*, **67** (9) 1823–1829 (2007)
29. Vähä-Nissi, M, Kervinen, K, Savolainen, A, Egolf, S, Lau, W, ''Hydrophobic Polymers as Barrier Dispersion Coatings.'' *Appl. Polym. Sci.*, **101** (3) 1958–1962 (2005)
30. Andersson, C, Marie, E, Järnström, L, ''Barrier Properties and Heat Sealability/Failure Mechanisms of Dispersion-Coated Paperboard.'' *Package. Technol. Sci.*, **15** (4) 209–224 (2002)
31. Kugge, C, Johnson, B, ''Improved Barrier Properties of Double Dispersion Coated Liner.'' *Prog. Org. Coat.*, **62** (4) 430–435 (2008)
32. Zhu, Y, Bousfield, D, Gramlich, W, ''The Influence of Pigment Type and Loading on Water Vapor Barrier Properties of Paper Coatings Before and After Folding.'' *Prog. Org. Coat.*, **132** 201–210 (2019)
33. Martinez-Hermosilla, G, Mesic, B, Bronlund, J, ''A Review of Thermoplastic Composites Vapour Permeability Models: Applicability for Barrier Dispersion Coatings.'' *Package. Technol. Sci.*, **28** (7) 565–578 (2015)
34. Nielsen, L, ''Models for the Permeability of Filled Polymer Systems.'' *J. Macromol. Sci.*, **1** (5) 929–942 (1967)